OPTIMIZED FAST HANKEL TRANSFORM FILTERS[1]

NIELS BØIE CHRISTENSEN[2]

ABSTRACT

CHRISTENSEN, N.B. 1990. Optimized fast Hankel transform filters. *Geophysical Prospecting* **38**, 545–568.

In the linear digital filter theory for calculation of Hankel transforms it is possible to find explicit series expansions for the filter coefficients. A method is presented for optimizing the Hankel filters calculated in this way. For a certain desired accuracy of computation, the sampling density and filter length are minimized by choosing the parameters determining the filter characteristics according to the analytical properties of the input function. A new approach to the calculation of the filter coefficients has been developed for these optimized filters. The length of the filters may be further reduced by introducing a shift in the sampling scheme.

INTRODUCTION

The linear filter method for calculation of Hankel transforms has been the subject of numerous papers in the geophysical literature since its introduction by Ghosh (1971a, b). Since it was realized that, compared with methods of numerical integration, a substantial reduction in computation time could be achieved, many contributions have been made to developing the method. The first papers on the subject focussed on short filters with a very limited number of coefficients (Ghosh 1971a, b; Das, Ghosh and Biewinga 1974; Das and Ghosh 1974), but the widespread use of fast digital computers in the 1970s turned the emphasis to methods of computing longer filters with the order of 100 coefficients (Koefoed, Ghosh and Polman 1972; Johansen 1975).

Some authors obtained the filter coefficients by direct integration of the convolution integral containing the interpolating sinc function and the Bessel function (Bichara and Lakshmanan 1976; Bernabini and Cardarelli 1978). Most common, however, was the use of a Hankel transform function pair in the generation of the filter coefficients. Filters calculated in this way depend on the choice of generating functions, and the accuracy in their application can be determined from numerical experiments only. This approach probably reached its height with the paper by Anderson (1979), where he presents a FORTRAN computer routine capable of per-

---

forming a Hankel transform of order 0 and 1. This routine has found widespread use. Recently a hybrid program of digital filtering and numerical integration has been published (Anderson 1989).

However, Johansen and Sørensen (1979), henceforth referred to as J&S, obtained explicit series expansions of the filter coefficients and, most importantly found a majorant for the error in the application of the filters. This paper is a further development of this approach.

RECAPITULATION OF THE METHOD

The following two paragraphs are a review of the method of J&S.
We consider the Hankel integral

$$g(r) = \int_0^\infty f(\lambda)\lambda J_\nu(\lambda r) \, d\lambda, \qquad \nu > -1. \tag{1}$$

By the substitutions

$$\lambda = \exp(-u), \qquad r = \exp(v), \tag{2}$$

and the definitions

$$F(u) = \exp(-u)f(\exp(-u)),$$

$$G(v) = \exp(v)g(\exp(v)), \tag{3}$$

$$H(u) = \exp(u)J_\nu(\exp(u)),$$

(1) may be rewritten as a convolution integral:

$$G(v) = \int_{-\infty}^\infty F(u)H_\nu(v-u) \, du \qquad \text{or} \qquad G = F * H_\nu. \tag{4}$$

Using the convolution theorem we find

$$\hat{G}(s) = \hat{F}(s) \times \hat{H}_\nu(s), \tag{5}$$

where

$$\hat{H}_\nu(s) = \int_{-\infty}^\infty H_\nu(v) \exp(-i2\pi vs) \, dv, \tag{6}$$

and analogously for $\hat{F}$ and $\hat{G}$.
$\hat{H}_\nu(s)$ may be evaluated explicitly:

$$\hat{H}_\nu(s) = 2^{-i2\pi s} \frac{\Gamma\left(\dfrac{\nu+1}{2} - i\pi s\right)}{\Gamma\left(\dfrac{\nu+1}{2} + i\pi s\right)}, \tag{7}$$

and has the property $|\hat{H}_\nu(s)| \equiv 1$, s real.

The numerical problem of calculating $G(v)$ is formulated by substituting the function F^* defined by

$$F^*(u) = \sum_{-\infty}^{\infty} F(n\Delta)P\left(\frac{u}{\Delta} - n\right),$$ (8)

which is the sampled and interpolated version of F, into (4), which then gives us the approximation G^* to G

$$G^*(v) = \int_{-\infty}^{\infty} F^*(u)H_v(v - u)\, du,$$

$$= \sum_{-\infty}^{\infty} F(n\Delta)H_v^*(v - n\Delta),$$ (9)

with

$$H_v^*(v) = \int_{-\infty}^{\infty} P\left(\frac{u}{\Delta}\right)H_v(v - u)\, du = P\left(\frac{u}{\Delta}\right) * H_v(u).$$ (10)

Considering only values of $v = m\Delta$, m integer, we have

$$G^*(m\Delta) = \sum_{-\infty}^{\infty} F(n\Delta)H_v^*[(m - n)\Delta].$$ (11)

G^* is thus obtained at discrete points as a discrete convolution between sampled values of F and the filter coefficients $H_v^*(k\Delta)$, k integer. We may then construct an approximation $G^{**}(v)$ to $G(v)$ by the usual interpolation scheme

$$G^{**}(v) = \sum_{-\infty}^{\infty} G^*(m\Delta)P'\left(\frac{v}{\Delta} - m\right).$$ (12)

P and P' are interpolating functions in (8) and (12).

The filter coefficients $H_v^*(v)$ may be calculated by using the convolution theorem on (10):

$$H_v^*(v) = \int_{-\infty}^{\infty} \Delta\hat{P}(\Delta s)\hat{H}_v(s)\exp(i2\pi vs)\, ds,$$ (13)

and by introducing the interpolating/filter function transform pair

$$P(u) = a\,\frac{\sin(\pi u)}{\sinh(\pi au)} = \text{sinsh}(u)$$ (14)

$$\hat{P}(s) = \tfrac{1}{2}\tanh\left[\frac{\pi}{a}(s + \tfrac{1}{2})\right] - \tfrac{1}{2}\tanh\left[\frac{\pi}{a}(s - \tfrac{1}{2})\right].$$ (15)

Figure 1 shows the filter function $\hat{P}(s)$ and the interpolating function $P(u)$ for different values of the smoothness parameter a.
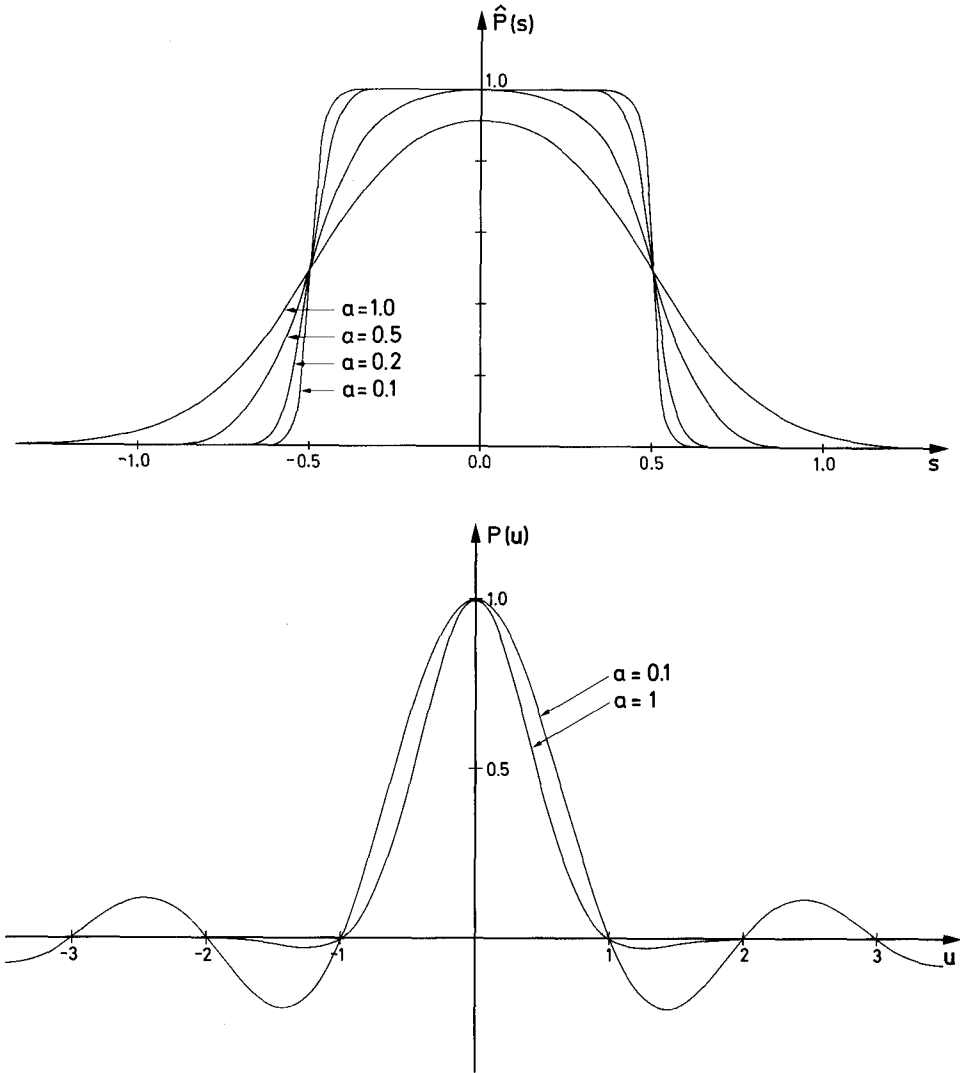
FIG. 1. The filter function $\hat{P}(s)$, s real, and the interpolating function $P(u)$ for different values of the smoothness parameter a.

$H_v^*(v)$ is computed as a contour integral in the complex $\xi = s + i\sigma$ plane (Fig. 2). The expressions for $H_v^*(v)$ as sums of residues are derived in Appendix A. Here only the key points will be mentioned.

$\hat{H}_v(\xi)$ decreases faster than any exponential function in the lower half-plane as $\sigma \to -\infty$ and $\hat{P}(\xi)$ decreases exponentially as $|s| \to \infty$, and thus the expression for $H_v^*(v)$ as a sum of residues in the lower half-plane is convergent for all v. However, the expression is used only for $v < v^-$, $(v^- = 0)$, since for $v > v^-$, the summation of
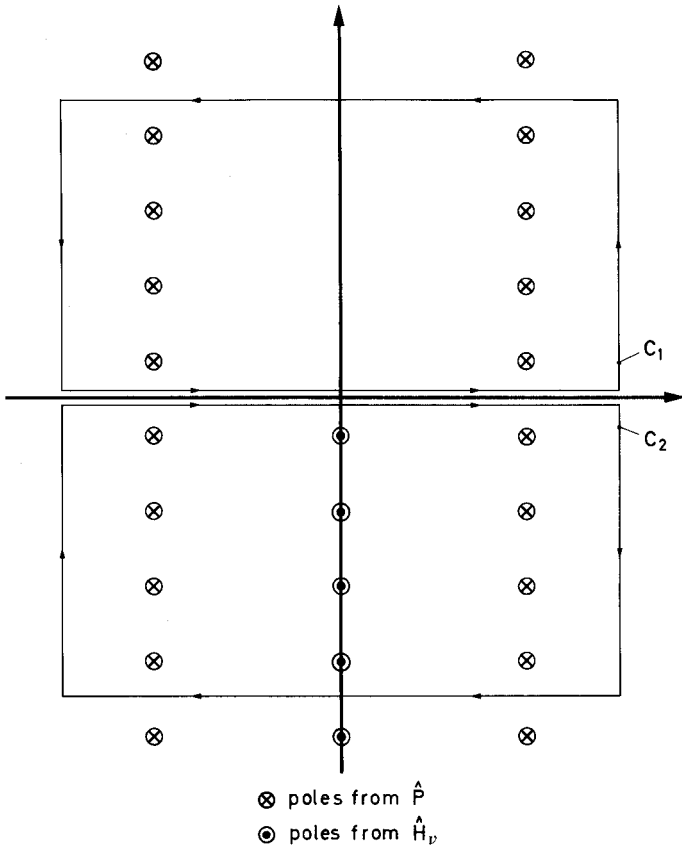
⊗ poles from $\hat{P}$

⊙ poles from $\hat{H}_{\nu}$

FIG. 2. The position of the poles of $\hat{H}_{\nu}(\xi)$ and of $\Delta\hat{P}(\Delta\xi)$ and the integration paths C_1 and C_2 in the lower and upper half-plane, respectively.

numerically large complex terms with alternating phase results in loss of accuracy. The resulting expression is given by

$$H_{\nu}^{*}(v) = 2^{-\nu} \exp\left[(\nu + 1)v\right] \sum_{n=0}^{\infty} \frac{(-1)^{n}}{4^{n}\Gamma(n+1)\Gamma(n+\nu+1)} \exp\left(2n v\right) \Delta\hat{P}(\Delta z_{n})$$

$$- 2a \exp\left(2\pi a s_{c}\, v\right) \operatorname{Im}\left\{\exp\left(i2\pi s_{c}\, v\right) \sum_{n=0}^{\infty} \exp\left(4\pi a s_{c}\, n v\right)\hat{H}_{\nu}(\xi_{n}^{-})\right\}, \qquad (16)$$

where

$$s_{c} = \frac{1}{2\Delta}, \qquad z_{n} = -\frac{i}{\pi}\left(n + \frac{\nu+1}{2}\right), \qquad \xi_{n}^{\pm} = s_{c} \pm i2a s_{c}(n + \tfrac{1}{2}).$$

For $v > v^{+}$, the integral is approximated by a sum over residues in the upper half-plane. Though $\hat{H}_{\nu}(\xi)$ increases faster than any exponential function as $\sigma \to \infty$,

the effect of the exponential factor in the integrand of (13) is to introduce a 'valley' in which we may place the return path of the contour. The depth of the valley increases with increasing v, and thus there exists a v^+ so that the integral through the valley becomes negligible $(< 10^{-16})$ for $v > v^+$.

For $v > v^+$ we find the following expression:

$$H_v^*(v) = 2a \exp\left(-2\pi a s_c v\right) \operatorname{Im}\left\{\exp\left(i2\pi s_c v\right) \sum_{n=0}^{N} \exp\left(-4\pi a s_c nv\right) \hat{H}_v(\xi_n^+)\right\}, \quad (17)$$

where N is the number of poles included in the summation.

The valley of the return path is a very deep and wide one, and thus the condition that the error integral through the valley must be negligible has the consequence of truncating the summation in (17) long before the valley bottom is reached for any reasonable desired relative accuracy of $H_v^*(v)$, e.g. 10^{-12}.

In the interval $v^- < v < v^+$, computation is performed by multiplying the integrand of (13) with an 'annihilator' function $\hat{Q}(\xi)$, given by

$$\hat{Q}(\xi) = \left\{1 + \exp\left[-\frac{i2\pi}{b}(\xi - i\sigma_c)\right]\right\}^{-1}, \quad (18)$$

which for properly chosen b and σ_c is sufficiently close to 1 on the real axis to have a negligible influence on $H_v^*(v)$ and which introduces an additional exponential decay as $\sigma \to \infty$. This will make the valley deep enough for the integral through the return path to be negligible. The price paid for this is the introduction of an additional row of poles on the line $\sigma = \sigma_c$, which must be taken into account together with the poles from $\hat{P}$ in the upper half-plane (Fig. 3).

ERROR ESTIMATION

J&S have shown how the absolute error in the calculation of G^* may be evaluated as

$$|G(v) - G^*(v)| \le 2 \int_{-\infty}^{\infty} |\hat{F}(s)| [1 - \hat{P}(\Delta s)] \, ds, \quad (19)$$

and by applying the spectrum majorization theorem to $F(u)$, we find that

$$|\hat{F}(s)| \le K(\omega_0) \times \exp\left(-2\pi\omega_0 |s|\right), \quad (20)$$

and

$$K(\omega_0) = \max \int_{0}^{\infty} |f(\lambda \exp\left(\pm i\omega_0\right))| \, d\lambda, \quad (21)$$

where $f(\lambda e^{i\omega})$ is analytic within the area $|\omega| < \omega_\sigma$.

Inserting (20) in (19) and evaluating the integral we obtain

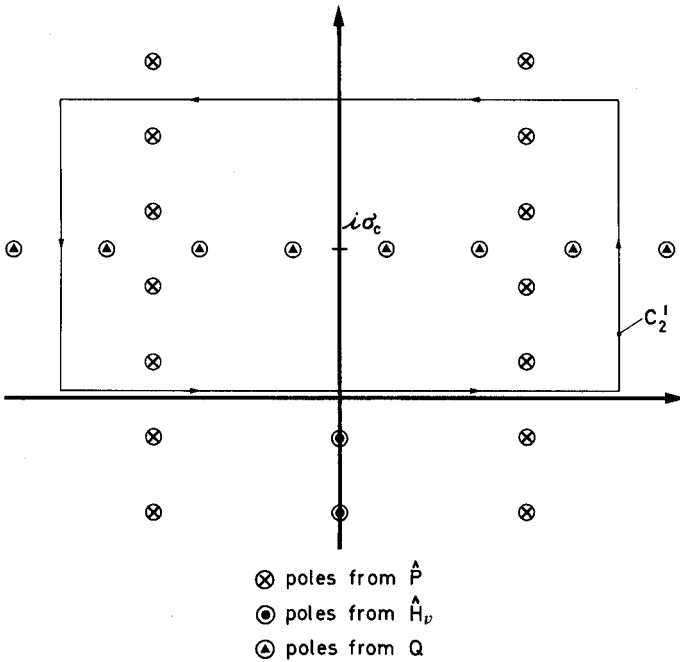$$|G(v) - G^*(v)| \le 4 \times K(\omega_0) \times E(\omega_0, a, s_c) \quad (22)$$

FIG. 3. As Fig. 2, but with the position of the poles of $\hat{Q}(\xi)$ added. The integration path in the upper half-plane is shown.

where $K(\omega_0)$ is given by (21) and

$$E(\omega_0, a, s_c) = \frac{as_c}{\sin{(2\pi as_c \, \omega_0)}} \exp{(-2\pi\omega_0 s_c)}$$

$$+ \frac{(2as_c \, \omega_0)^2}{\pi\omega_0} \sum_{p=1}^{\infty} (-1)^p \frac{\exp{(-p\pi/a)}}{p^2 - (2as_c \, \omega_0)^2}. \qquad (23)$$

In J&S the value of the smoothness parameter a is subjected to the restriction $2\pi as_c = 1/M$, $M = 1, 2, 3, \ldots$. This makes it possible to discard certain terms in the summation of residues from the poles of $\hat{H}_\nu(\xi)$.

MAIN FEATURES OF THE METHOD

There are four points to be made concerning the Hankel filters developed by Johansen and Sørensen.

(1) It is possible to estimate the error. For a given input function $f(\lambda)$, the opening angle of the region of analyticity determines $K(\omega_0)$, and we may find a cut-off frequency s_c and a smoothness parameter a, such that $|G(v) - G^*(v)| < \varepsilon$ for a given ε. Practically, two problems arise. Firstly, we are generally interested in an estimate for a class of input functions, for example input functions from geoelectrical

soundings over a horizontally stratified earth. It turns out that $K(\omega_0)$ is strongly dependent on the model assumed, so we must evaluate $K(\omega_0)$ for a whole class of earth models. Secondly, it may be rather difficult to evaluate $K(\omega_0)$ for any model of interest. However, numerical experiments may give an estimate of the 'effective' $K(\omega_0)$ defined by

$$K_{eff}(\omega_0) = \frac{\max |G(v) - G^*(v)|}{4E(\omega_0, a, s_c)}. \tag{24}$$

Let us assume that we have made computations with two different filters, one with a very dense sampling scheme (suffix 0), and one with a more sparse sampling density (suffix 1). We then have

$$K_{eff}(\omega_0) = \frac{\max |G(v) - G_1^*(v)|}{4E_1} \approx \frac{\max |G_0^*(v) - G_1^*(v)|}{4E_1}. \tag{25}$$

These calculations must be done for a representative class of models. In the case of geoelectrical soundings a number of two- and three-layer models with relevant resistivity contrasts and layer thicknesses must be considered.

(2) The error decreases exponentially with the cut-off frequency s_c. This means that even a moderate increase in sampling density will make the error decrease drastically. An increase in sampling density of one sample per decade will make the error majorant decrease by a factor of 73, corresponding to nearly two digits for $\omega_0 = \pi$ (analytic input functions). For $\omega_0 = \frac{1}{2}\pi$ (d.c. geoelectric soundings) the error majorant decreases by a factor of 8.5, which will give approximately one more digit, and for $\omega_0 = \frac{1}{4}\pi$ (electromagnetic problems) the error majorant decreases by a factor of 3.

(3) The filter coefficients decrease exponentially as $|v| \to \infty$. This is an important property of the Hankel filters constructed in this way, since it restricts the discrete convolution to a limited interval.

Let $2\pi a s_c = 1/M$, $M = 1, 2, 3, \dots$. As $v \to \infty$, (17) becomes

$$H_v^*(v) \sim \exp(-2\pi a s_c v) = \exp\left(-\frac{v}{M}\right), \tag{26}$$

while for $v \to -\infty$ (16) becomes

$$H_v^*(v) \sim \exp(2\pi a s_c v) = \exp\left(\frac{v}{M}\right) \quad \text{or} \quad H_v^*(v) \sim \exp[(v + 1)v], \tag{27}$$

whichever decays the slowest.

We see that a smaller a (greater M), corresponding to a sharper cut-off of the filter function $\hat{P}$, results in a slower decay of the filter.

(4) The filter coefficients $H_v^*(v)$ are accurate. The filter coefficients are expressed as series expansions, which makes it possible to evaluate them to any desired accuracy, which also means that they actually decay exponentially as mentioned in point (3). In contrast to this, filter coefficients generated by use of the FFT routine will asymptotically reach a certain numerical 'noise level' below which they

will not decrease. Besides round-off errors of the input function and the discrete convolution, and truncation errors, this introduces an additional source of error in the output function, which may be of importance in case of high accuracy computations. However, the importance of this depends on the representation error of the computer used.

ANALYSIS OF THE ERROR EXPRESSION $E\,(\omega_0,\,a,\,s_c)$

In J&S the smoothness parameter a of the filter function $\hat{P}$ was restricted by the choice

$$2\pi a s_c = \frac{1}{M}, \qquad M = 1, 2, 3, \ldots. \tag{28}$$

From the asymptotic behaviour of the filters mentioned in the previous section, we see that this means that the filter cannot decay faster than $\exp(-v)$ as $v \to \infty$, corresponding to $M = 1$. For $M > 1$, the situation is worse. With increasing M, the oscillations of the tails of the filter persist longer. Hence we wish to choose a value of a greater than that permitted by (28), thus making the filter decay faster as $v \to \infty$. As $v \to -\infty$, the filter cannot decay faster than $\exp[(v + 1)v]$, but we can take full advantage of this by choosing a so that $2\pi a s_c > v + 1$. However, choosing a greater value of a might have serious consequences for the error expression $E(\omega_0, a, s_c)$ so let us examine this expression as a function of a.

From (23)

$$E(\omega_0, a, s_c) = \frac{as_c}{\sin(2\pi a s_c \omega_0)} \exp(-2\pi\omega_0 s_c)$$

$$+ \frac{(2as_c \omega_0)^2}{\pi\omega_0} \sum_{p=1}^{\infty} (-1)^p \frac{\exp(-p\pi/a)}{p^2 - (2as_c \omega_0)^2}. \tag{29}$$

The two terms both have singularities for $2as_c \omega_0 = n$, $n = 1, 2, 3, \ldots$, but it can be shown that the singularities cancel each other thus making $E(\omega_0, a, s_c)$ continuous.

Outside the singularities we find

$$\lim_{s_c \to \infty} E(\omega_0, a, s_c) = E_{\min}(\omega_0, a) = \exp\left(-\frac{\pi}{a}\right)/\pi\omega_0. \tag{30}$$

This is what we see in Fig. 4. For a given a, we cannot make the error smaller than $E_{\min}(\omega_0, a)$ given by (30). We observe that a greater a corresponds to a greater $E_{\min}(\omega_0, a)$. Furthermore, for a given a, permitting $E(\omega_0, a, s_c)$ to be smaller than a desired accuracy, there is no point in choosing s_c greater than a value around the 'knee' of the curve $E(\omega_0, a, s_c)$. Choosing $s_c = 1/2a\omega_0$, corresponding to the first singularity in (29), places s_c at this 'knee' point.

We may use the following procedure for the determination of a and s_c:

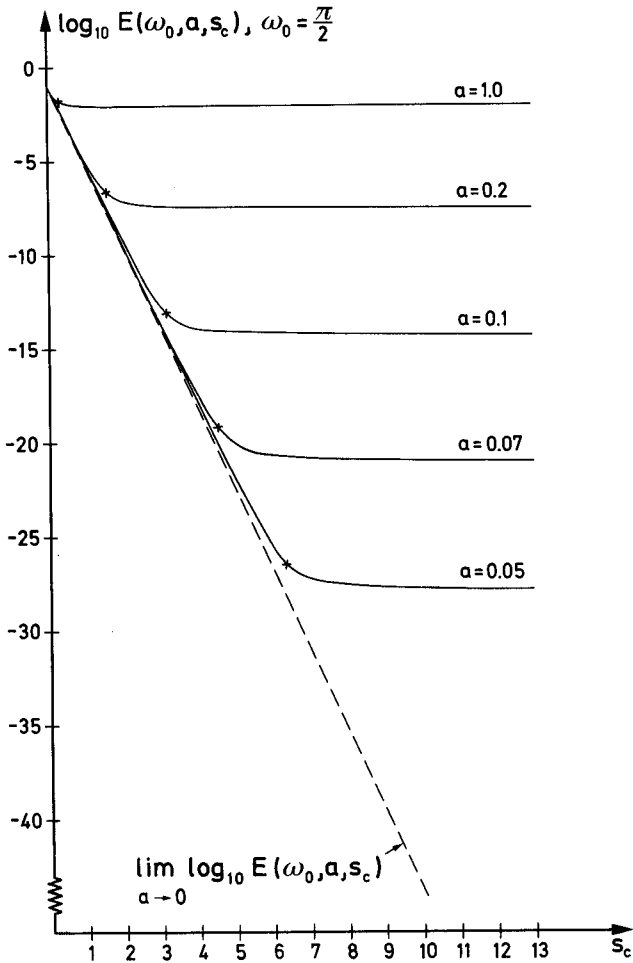(1) The analytical properties of the input function $f(\lambda)$ determine ω_0.

FIG. 4. The error expression $E(\omega_0, a, s_c)$ as a function of s_c for different values of the smoothness parameter a. The points corresponding to optimized filters are marked with a cross.

(2) Having estimated $K(\omega_0)$, we specify $E(\omega_0, a, s_c) < \varepsilon$ in order to calculate $G^{**}(v)$ to a certain desired accuracy.

(3) We choose the greatest possible value of a, so that $E(\omega_0, a, s_c) < \varepsilon$ at the 'knee' point.

(4) We choose $s_c = 1/2a\omega_0$.

In order to perform step (3), we need an expression for $E(\omega_0, a, s_c)$ at $s_c = 1/2a\omega_0$. On taking limits, we find

$$E(\omega_0, s_c) = \left(s_c + \frac{1}{4\pi\omega_0}\right) \exp\left(-2\pi s_c \omega_0\right)$$

$$+ \frac{1}{\pi\omega_0} \sum_{p=2}^{\infty} (-1)^n \frac{\exp\left(-2\pi s_c \omega_0 p\right)}{p^2 - 1}, \qquad 2as_c \omega_0 = 1, \qquad (31)$$

or in terms of a,

$$E(\omega_0, a) = \left(\frac{1}{2a\omega_0} + \frac{1}{4\pi\omega_0}\right) \exp\left(-\frac{\pi}{a}\right)$$

$$+ \frac{1}{\pi\omega_0} \sum_{p=2}^{\infty} (-1)^p \frac{\exp\left(-\frac{p\pi}{a}\right)}{p^2 - 1}, \qquad 2as_c\,\omega_0 = 1. \tag{32}$$

For $a \leq 1$ (i.e. $s_c \geq 1/2\omega_0$), the terms involved in the sums in (31) and (32) are smaller than 1% of the main terms and may therefore be discarded giving

$$E(\omega_0, s_c) \approx \left(s_c + \frac{1}{4\pi\omega_0}\right) \exp\left(-2\pi s_c\,\omega_0\right), \qquad s_c \geq \frac{1}{2\omega_0}, \tag{33}$$

$$E(\omega_0, a) \approx \left(\frac{1}{2a\omega_0} + \frac{1}{4\pi\omega_0}\right) \exp\left(-\frac{\pi}{a}\right), \qquad a \leq 1. \tag{34}$$

Figure 5 shows $E(\omega_0, s_c)$ as a function of s_c. The exponential decay with s_c is retained. From (31) and (29) we find that the quotient of the error for optimized filters and the asymptotic value of the error, as $a \to 0$, is

$$\frac{E(\omega_0, s_c)}{\lim_{a \to 0} E(\omega_0, a, s_c)} \approx 2\pi\omega_0 s_c + \tfrac{1}{2}$$

which typically attains a value between 10 and 50.

Filters constructed in this way will be called 'optimized filters' for the following reason: For a given accuracy, a is chosen as large as possible thus making the filter as short as possible, and s_c is chosen as small as possible thus reducing the calculation of $F(n\Delta)$ to a minimum.

Figure 6 shows optimized J_0 filters ($2as_c\,\omega_0 = 1$) where $s_c = 1.25$ and $\omega_0 = \pi, \tfrac{1}{2}\pi$, and $\tfrac{1}{4}\pi$. We see that the oscillating end of the filter becomes increasingly damped as ω_0 gets smaller (a becomes greater), while the left side remains unchanged.

It is interesting to see the effect of this choice of a and s_c on the filter function $\Delta\hat{P}(\Delta s)$.

Substituting $2as_c\,\omega_0 = 1$ in the asymptotic expansion for $\Delta\hat{P}(\Delta s)$ we find

$$\Delta\hat{P}(\Delta s) \sim \exp\left(-\frac{2\pi|s|}{2as_c}\right) = \exp\left(-2\pi\omega_0|s|\right), \qquad |s| \to \infty. \tag{35}$$

The exponential decay of the filter function $\Delta\hat{P}(\Delta s)$ for large $|s|$ is thus identical to the exponential decay of the majorant for $|\hat{F}(s)|$ given in (20).

CALCULATION OF $H_\nu^*(v)$ FOR ARBITRARY a

We need to devise a method for calculating the filter coefficients $H_\nu^*(v)$ without the previously imposed restriction on a in (28).

For $v < v^-$ we shall use the full expression of (16). The approximated expression of J&S may no longer be used, as we have abandoned the restriction $2\pi as_c = 1/M$,
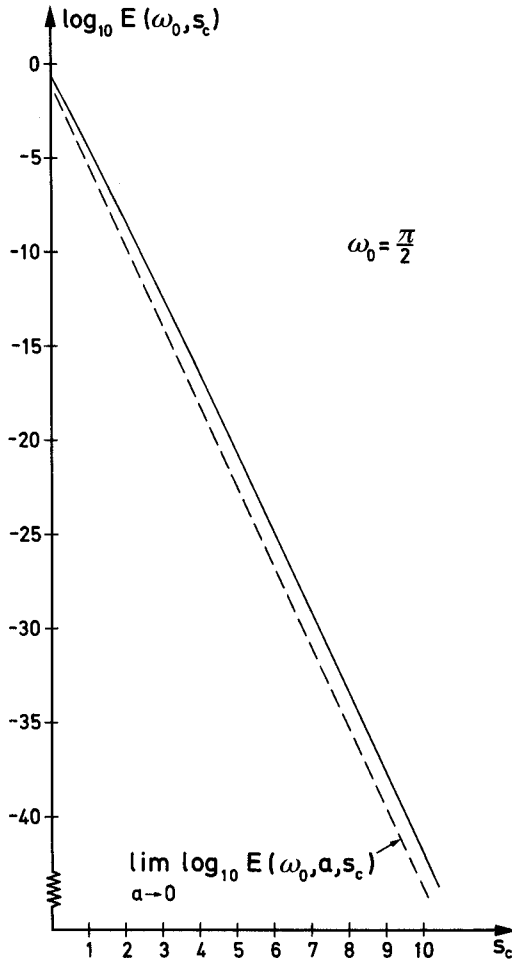
FIG. 5. The error expression $E(\omega_0, s_c)$ for optimized filters as a function of s_c.

$M = 1, 2, 3, \ldots$. The resulting sums are numerically stable for $v < \ln 2$, so we may choose $v^- = \ln 2$ and use (16).

For $v > v^+$, (17) is used unchanged. Theoretical investigation of the error integral through the 'valley', combined with numerical experiments, shows that the choice of $v^+ = 4 + 0.1s_c$ will make the error integral through the valley smaller than 10^{-16}.

In the interval $v^- < v < v^+$, we shall develop an alternative way of computing $H_v^*(v)$.

Using the convolution theorem on (10) we get

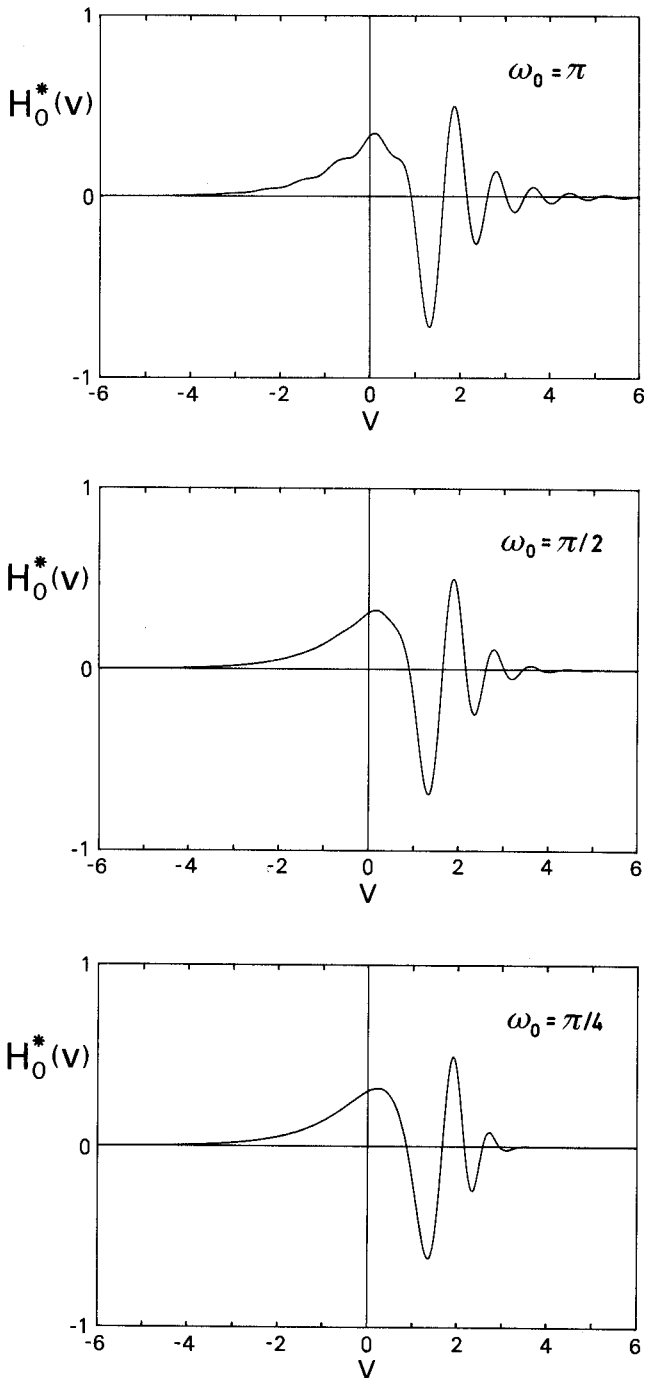$$\hat{H}_v^*(s) = \hat{H}_v(s) \times \Delta\hat{P}(\Delta s). \tag{36}$$

FIG. 6. Optimized J_0-filters for $s_c = 1.25$ and for $\omega_0 = \pi$, $\frac{1}{2}\pi$ and $\frac{1}{4}\pi$.

Now we construct the generalized function

$$\hat{\mathscr{H}}^*_\nu(s) = \hat{H}^*_\nu(s) \times \frac{1}{\Delta_1} \, \text{III}\!\left(\frac{s}{\Delta_1}\right), \tag{37}$$

where $\text{III}(s)$ is the 'shah' function (Bracewell 1965) defined by

$$\text{III}(s) = \sum_{-\infty}^{\infty} \delta(s - n). \tag{38}$$

$\hat{\mathscr{H}}^*_\nu(s)$ is thus a sampled version of $\hat{H}^*_\nu(s)$.

The convolution theorem gives us

$$\mathscr{H}^*_\nu(v) = \int_{-\infty}^{\infty} \hat{\mathscr{H}}^*_\nu(s) \exp{(i2\pi vs)} \, ds,$$

$$= H^*_\nu(v) * \text{III}(\Delta_1 v),$$

$$= \frac{1}{\Delta_1} \sum_{-\infty}^{\infty} H^*_\nu\!\left(v - \frac{n}{\Delta_1}\right). \tag{39}$$

On the other hand,

$$\mathscr{H}^*_\nu(v) = \int_{-\infty}^{\infty} \hat{H}_\nu(s) \times \Delta\hat{P}(\Delta s) \times \frac{1}{\Delta_1} \, \text{III}\!\left(\frac{s}{\Delta_1}\right) \exp{(i2\pi vs)} \, ds,$$

$$= \sum_{-\infty}^{\infty} \Delta\hat{P}(n\Delta\Delta_1)\hat{H}_\nu(n\Delta_1) \exp{(i2\pi vn\Delta_1)}. \tag{40}$$

Combining (39) and (40) and splitting the term with $n = 0$ from the rest of the summation in (39), we finally arrive at

$$H^*_\nu(v) = \Delta_1 \sum_{-\infty}^{\infty} \Delta\hat{P}(n\Delta\Delta_1)\hat{H}_\nu(n\Delta_1) \exp{(i2\pi vn\Delta_1)}$$

$$- \sum_{n=1}^{\infty} H^*_\nu\!\left(v - \frac{n}{\Delta_1}\right) - \sum_{n=1}^{\infty} H^*_\nu\!\left(v + \frac{n}{\Delta_1}\right). \tag{41}$$

We see that $H^*_\nu(v)$ is expressed as a discrete Fourier sum minus sums of filter coefficients of arguments to the left and right of v.

Choosing Δ_1 so small that $v - (1/\Delta_1) < v^-$ and $v + (1/\Delta_1) > v^+$ for all $v^- < v < v^+$, (41) enables us to calculate $H^*_\nu(v)$ in the range $v^- < v < v^+$. $1/\Delta_1 = (v^+ - v^-)$ gives the greatest value of Δ_1 meeting this demand and is thus the best one, as a smaller Δ_1 would result in denser sampling on the real axis of $\Delta\hat{P}(\Delta s)\hat{H}_\nu(s)$.

Compared with the method of J&S, we see that the new expression has transformed the sampling of $\Delta\hat{P}(\Delta s)\hat{H}_\nu(s)$ on the line $\sigma = \sigma_c$ (at the poles of $\hat{Q}(\xi)$, Fig. 3) to a sampling on the real axis. The Fourier sum in (41) converges as $|n| \to \infty$. Remembering $|\hat{H}_\nu(s)| \equiv 1$, s real, the absolute value of the terms is equal to

$\Delta\hat{P}(n\Delta\Delta_1)$ which decreases exponentially (35) for values of the argument greater than approximately 1 (Fig. 1), i.e. $|n\Delta\Delta_1| > 1$.

To ensure speed of operation and numerical stability, the summation of coefficients with arguments to the left and right of v is done by inserting the summations giving $H_v^*(v)$ for $v < v^-$ and for $v > v^+$ in (41). The resulting double summations can be reduced to only one summation by changing the order of summations, as the summation over n in (41) becomes the sum of a geometric progression, which is expresssible in closed form.

IMPLEMENTATION OF THE PROGRAM

As can be seen from (16), (17) and (41), only elementary functions enter in the expressions for $H_v^*(v)$ except for $\hat{H}_v(\xi)$ which contains the complex gamma function $\Gamma(\xi)$. With respect to the elementary functions, certain precautions have to be taken concerning the numerical accuracy for special values of the arguments, but no more than in ordinary programming procedures. The complex gamma function is calculated using the asymptotic expansion (Abramowitz and Stegun 1970, eq. 6.1.40). Retaining six terms in the series with Bernoulli number coefficients will ensure an absolute accuracy of the logarithm of the gamma function smaller than 10^{-12} for arguments numerically greater than 6.6. For smaller arguments, an integer is added to make the absolute value greater than 6.6, and the correct value is then obtained using the recursion formula $\Gamma(1 + z) = z\Gamma(z)$.

The number of residues to be added is quite small. Inspection of (16), (17) and (41) shows that the residues entering as coefficients in the power series are independent of v, so need only be calculated once for a given set of filter parameters v, s_c, a. For optimized filters, the maximum number of terms to be added for any v, any v, $0.5 < s_c < 10$, and $\frac{1}{2}\pi < \omega_0 < \pi$ is:

  – on the negative imaginary axis, 12
  – on the lines $|s| = s_c$ in the lower half-plane, 9
  – on the lines $|s| = s_c$ in the upper half-plane, 18
  – on the real axis, 95.

Computational time is approximately 0.5–1 s for calculating the coefficients needed in the power series and thereafter approx. 10 ms per filter coefficient for $v < v^-$ and for $v > v^+$, while for any filter coefficient with $v^- < v < v^+$, the computational time is approx. 50 ms. A set of 200 filter coefficients can thus be calculated in less than 5 s. Computation times refer to a NORD 110 mini computer, but most modern PCs are as fast.

A FORTRAN77 program has been written to calculate filter coefficients for any choice of parameters. A subroutine performs the convolution with a J_0 and/or a J_1 filter. A user complex input function must be supplied together with the interval over which the convolution is to be evaluated. The routine minimizes the number of calls to the input function by saving previously calculated values. A similar routine performing cosine and sine transforms is available. These programs will be sent on request on a $5\frac{1}{4}''$ floppy disc in DOS format, so no filter coefficients will be given here.

EVALUATION OF OPTIMIZED FILTERS

The question now arises as to whether optimized filters are an improvement on the old ones.

Firstly, optimized filters retain all the required characteristics (1)–(4) in the section: Main features of the method, and they represent an improvement in (3). The optimized filters decay faster than the old ones in one direction ($v \to \infty$) while in the other direction ($v \to -\infty$) the filters may or may not provide improvement since they cannot decay faster than $\exp[(1 + v)v]$. From the convolution expression

$$G^*(v) = \int_{-\infty}^{\infty} F^*(u) H_v(v - u) \, du \qquad (42)$$

we see that $(v - u) \to \infty$ for a given v corresponding to $u \to -\infty$, i.e. $\lambda \to \infty$ in $f(\lambda)$. If $f(\lambda) \sim \exp(-\alpha\lambda)$ as $\lambda \to \infty$, then $F(u) \sim \exp(-\alpha e^{-u})$ as $u \to -\infty$, which shows that $F(u)$ drops rapidly to zero as $u \to -\infty$, and the length of the discrete convolution is determined mainly by the sharp cut-off of $F(u)$. In this case, the optimized filters are not a great improvement. However, if $f(\lambda) \sim$ constant, or if $f(\lambda) \sim \lambda^\mu$, $\mu > 0$, as $\lambda \to \infty$, then it is important that $H_v^*(v)$ rapidly approaches zero as $v \to \infty$. In addition integrals which are not absolutely convergent, i.e. $f(\lambda) \sim \lambda^\mu$, $\mu > 1/2$, as $\lambda \to \infty$, may be computed using the optimized filters. The calculations will give the

$$g(r) = \int_0^\infty \lambda e^{-\lambda} J_0(\lambda r) \, d\lambda = [1 + r^2]^{-3/2}$$

$$G(v) = rg(r) = r / [1 + r^2]^{3/2} \quad , \quad r = e^v$$
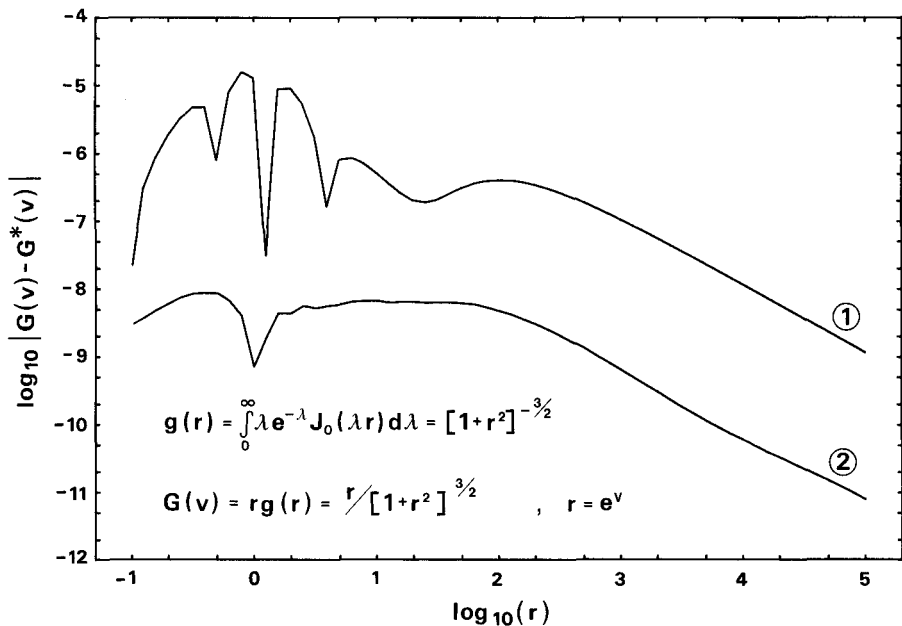
FIG. 7. The performance of the Hankel filters using the routine ZLAGH0 (Anderson 1982) (1) compared with the present Hankel filters (2) on an analytic input-output function pair. The sampling density of (1) is $\Delta = 0.2$ (≈ 11.5 samples per decade) while the sampling density of (2) is $\Delta = 0.23$ (10 per decade).

correct Cauchy principal value. In the preliminary phase of programming, one need not be concerned with separating the kernel function into a convergent and a non-convergent part, for example taking out the half-space response in geoelectrical soundings. Another example is the calculation of responses from d.c. marine electrical soundings, where source and receiver are placed at the same depth.

Figure 7 compares the performance of Hankel filters generated by the present method of series expansions, and Hankel filters generated by the FFT procedure using the FORTRAN routine ZLAGH0 (Anderson 1982) on an analytic input–output function pair. The figure shows the absolute error in $G(v)$, i.e. $|G(v) - G^*(v)| = r \times |g(r) - g^*(r)|$ since this is the expression which is evaluated in (22). We see that the error using the present filters is between one and two decades smaller than that produced by Anderson's filters although the sampling density is 15% smaller.

To illustrate that the optimized filters are capable of giving the correct Cauchy principal value, Fig. 8 shows the absolute error in $G(v)$ for two transforms, which are not absolutely convergent. Note that the factual error in $G(v)$ decreases as $\sim 1/r$.

Figures 7 and 8 illustrate a typical behaviour of the fast Hankel transform filters introduced in this paper. The error estimation only predicts that the absolute error in $G^*(v)$ will be smaller than a certain constant. The factual error, however, often decreases as $1/r$ as $r \to \infty$ and as r as $r \to 0$. This means that for exponentially decreasing output functions, the result of the discrete convolution will only reflect the error of the calculation and not the true value of the output function for large
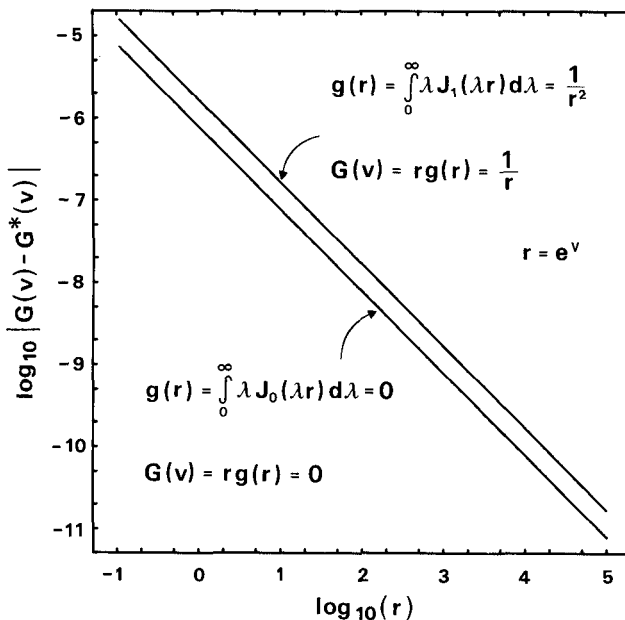

FIG. 8. The absolute error on $G(v)$ for two transforms which are not absolutely convergent. Sampling density is 10 per decade and optimized filters with $\omega_0 = \frac{1}{2}\pi$ have been used.

values of r. The present filters are thus not a remedy against the problems encountered in the calculation of the following integral (Goldman 1987) for large values of α:

$$g(r) = \int_0^\infty \frac{\lambda}{\sqrt{\lambda^2 + \alpha^2}} \, J_0(\lambda r) \, d\lambda = \frac{\exp(-\alpha r)}{r}.$$

Sampling at the Zeros of $H_\nu^*(v)$

In the early history of the filter method for Hankel transforms, one of the significant improvements consisted of sampling the filter function $H_\nu^*(v)$ at its zeros as $v \to \infty$, by introducing an appropriate shift in the sampling scheme. At that time, the filter coefficients decayed very slowly, as $H_\nu^*(v) \sim 1/v$ as $v \to \infty$ due to the use of the sinc-function instead of the 'sinsh' function (14) in the Fourier domain. The problem was analysed by Koefoed as early as 1972 and the shifting operation has been used by most authors since then. By sampling at the zeros of $H_\nu^*(v)$, a substantial reduction of the length of the filter was obtained. We may apply a similar method to the optimized filters, thus further reducing the length of the filters.

The convolution expression

$$G^*(v) = \int_{-\infty}^\infty F^*(u)H_\nu(v - u) \, du \tag{43}$$

may be rewritten as

$$G^*(v) = \int_{-\infty}^\infty F^*(u' + \Delta_0)H_\nu[(v - \Delta_0) - u'] \, du', \tag{44}$$

which, formulated discretely, becomes

$$G^*(m\Delta) = \sum_{-\infty}^\infty F(n\Delta + \Delta_0)H_\nu^*[(m - n)\Delta - \Delta_0], \tag{45}$$

and we see that we may introduce a shift Δ_0 in the sampling of $H_\nu^*(v)$ if we also introduce it in the sampling of $F(u)$, and still get the computed values at the previous sample points of $G^*(v)$.

For optimized filters, we have $2\pi a s_c = (\pi/\omega_0) \times 2as_c \omega_0 = (\pi/\omega_0) \geq 1$, thus the asymptotic decay of the filters given by (26) and (27) now reads

$$H_\nu^*(v) \sim \exp\left(-\frac{\pi}{\omega_0} v\right), \qquad v \to \infty, \tag{46}$$

$$H_\nu^*(v) \sim \exp\left(\frac{\pi}{\omega_0} v\right) \quad \text{or} \quad H_\nu^*(v) \sim \exp[(v + 1)v], \qquad v \to -\infty. \tag{47}$$

For $v \to -\infty$, the decay is controlled by $\exp[(v + 1)v]$ for $v + 1 < (\pi/\omega_0)$. However, as $v \to \infty$ and as $v \to -\infty$ in the case $v + 1 < (\pi/\omega_0)$, we may find a shift Δ_0 such that the filters will decay faster.

Let us consider the case $v \to \infty$. Retaining the first two terms in (17) we find

$$H_v^*(v) \approx 2a \exp(-2\pi a s_c v) \, \text{Im} \, \{\exp(i2\pi s_c v) \hat{H}_v(s_c + ias_c)\}$$

$$+ 2a \exp(-6\pi a s_c v) \, \text{Im} \, \{\exp(i2\pi s_c v) \hat{H}_v(s_c + i3as_c)\}. \tag{48}$$

Let $\hat{H}(s_c + ias_c) = Ae^{i\theta}$, and if the first term in (48) must be zero then

$$\text{Im} \, \{\exp(i2\pi s_c v) \times Ae^{i\theta}\} = 0 \Rightarrow$$

$$2\pi s_c v + \theta = p\pi, \qquad p \text{ integer} \Rightarrow$$

$$v = \left(p - \frac{\theta}{\pi}\right)\Delta, \qquad p \text{ integer}, \qquad \Delta = \frac{1}{2s_c}. \tag{49}$$

Thus we see that by choosing $\Delta_0 = -(\theta/\pi)(\Delta)$, we have determined a shift $|\Delta_0| < \Delta$ so that the first term in (48) is zero. The asymptotic behaviour of $H_v^*(v)$ is then determined by the second term, such that

$$H_v^*(v) \approx \exp(-6\pi a s_c v) \times 2a \, \text{Im} \, \{\exp(i2\pi s_c v) \hat{H}_v(s_c + i3as_c)\}$$

$$= \exp\left(-3\frac{\pi}{\omega_0}v\right) \times 2a \, \text{Im} \, \{\exp(i2\pi s_c v) \hat{H}_v(s_c + i3as_c)\} \tag{50}$$

for optimized filters. The exponent is thus three times greater for shifted filters than for non-shifted filters. For optimized filters with $\omega_0 = \pi$, this means that $H_v^*(v) \sim \exp(-3v)$ instead of $\exp(-v)$, with $\omega_0 = \frac{1}{2}\pi$ we have $H_v^*(v) \sim \exp(-6v)$ instead of $\exp(-2v)$, and with $\omega_0 = \frac{1}{4}\pi$ we find $H_v^*(v) \sim \exp(-12v)$ instead of $\exp(-4v)$.

Similarly, we may try to find a shift Δ_0' such that the first term in the sum of residues from the poles of $\Delta \hat{P}(\Delta s)$ in (16) vanishes for $v \to -\infty$, i.e.

$$2a \exp(2\pi a s_c v) \, \text{Im} \, \{\exp(i2\pi s_c v) \hat{H}_v(s_c - ias_c)\} = 0. \tag{51}$$

Observing that $\hat{H}_v(s_c - ias_c)$ is the complex conjugate of $[\hat{H}_v(s_c + ias_c)^{-1}]$, we have $\hat{H}_v(s_c - ias_c) = A^{-1}e^{i\theta}$ therefore we must have

$$\text{Im} \, \{\exp(i2\pi s_c v) \times A^{-1}e^{i\theta}\} = 0, \tag{52}$$

which leads to the same result as for $v \to \infty$. The shift Δ_0 which makes the sampling of $H_v^*(v)$ coincide asymptotically with its zeros for $v \to \infty$, thus also makes the sampling coincide with the zeros for $v \to -\infty$.

Just as for the optimization procedure, the shifting of the sampling points affects the filters mainly in one interval, as $v \to \infty$, while as $v \to -\infty$ the decay cannot be faster than $\exp[(v + 1)v]$ (47). The effect of shifting the filter is thus to enhance further the advantages of the optimization procedure, while no new aspects of improvement are introduced.

Figure 9 shows the rapid decay of the shifted optimized filters compared with non-shifted optimized filters. We see that the shifted filters decay 3 times faster (exponentially).

In the case of computer convolution routines customized to a special purpose the shifted filters will be advantageous. For more general purpose routines we may wish to use the same input function with different filters, and we must have the same
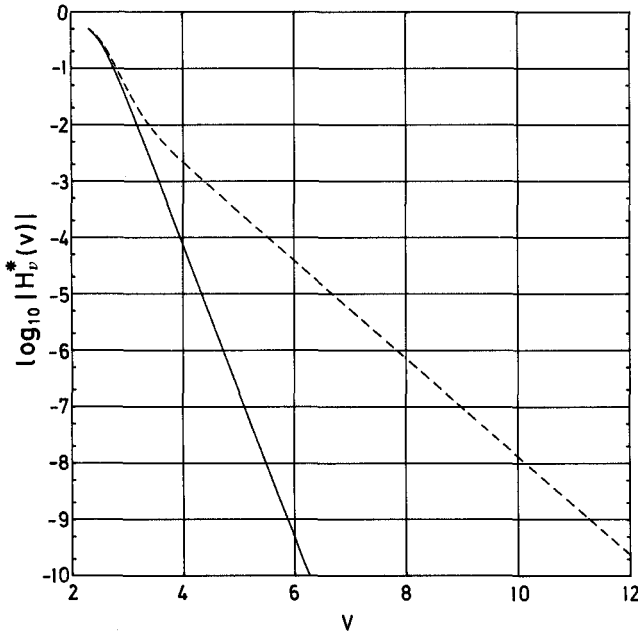
FIG. 9. The decay of shifted (———) and non-shifted (- - -) optimized J_0-filters for $\omega_0 = \frac{1}{2}\pi$ as $v \to \infty$.

sampling points for all filters in order to minimize the number of calls to the input function by using previously calculated values. The convolution routines written by the author (see previous section) use non-shifted optimized filters.

DISCUSSION

In an earlier section reasons were given why the present approach to the calculation of Hankel filters must be considered superior to the Fourier transform method on a generating function pair. The optimization procedure for Hankel filters presented here makes it possible to reduce the filter length. Under some circumstances, it may be possible to further reduce the filter length by introducing a shift in the sampling scheme of the filter coefficients.

Recent years have seen the presentation of new short filters (Guptasarma 1982; Nissen and Enmark 1986), and the logarithmic sampling scheme of the Hankel filters has also been applied in combination with FFT routines to the calculation of Fourier transforms (Haines and Jones 1988). New interest in short filters was evoked by the introduction of small personal computers and the growing interest in model calculations from two- and three-dimensional models in electromagnetic problems.

These new filters are generated by a least-squares procedure (Koefoed and Dirks 1979) where the 'best' set of coefficients using a certain number of points is sought, which will yield the correct Hankel transform of a certain input function. Again, the

coefficients depend on the choice of transform function pair, and the accuracy of their application can only be estimated numerically. They perform surprisingly well in most situations, better than other Hankel filters with the same number of coefficients. However, for high accuracy computations, where longer filters are required, the possibility of finding a global error limit of the calculations offered by the method presented here must be considered more important than the improvement in speed of the least-squares filters.

APPENDIX A

It will be here shown how the expressions (16) and (17) for $H_\nu^*(v)$ are found as sums of residues in the complex plane.

We shall calculate

$$H_\nu^*(v) = \int_{-\infty}^{\infty} \Delta\hat{P}(\Delta s)\hat{H}_\nu(s) \exp(i2\pi vs)\, ds, \tag{A1}$$

where

$$\hat{H}_\nu(s) = 2^{-i2\pi s}\, \frac{\Gamma\left(\dfrac{v+1}{2} - i\pi s\right)}{\Gamma\left(\dfrac{v+1}{2} + i\pi s\right)} \tag{A2}$$

and

$$\hat{P}(s) = \tfrac{1}{2}\tanh\left[\frac{\pi}{a}(s + \tfrac{1}{2})\right] - \tfrac{1}{2}\tanh\left[\frac{\pi}{a}(s - \tfrac{1}{2})\right]. \tag{A3}$$

$\hat{H}_\nu(\zeta)$, $\zeta = s + i\sigma$, is analytic except for the points $z_n = -(i/\pi)(n + \tfrac{1}{2}(v+1))$, $n = 0, 1, 2, \ldots$, where it possesses simple poles with the residues

$$R_n = i(-1)^n\, \frac{2^{-(2n+v+1)}}{\pi\Gamma(n+1)\Gamma(n+v+1)}. \tag{A4}$$

$\Delta\hat{P}(\Delta\zeta)$ is analytic except for the points $\zeta = \pm s_c + i2as_c(n + \tfrac{1}{2})$, $n = \cdots - 2, -1, 0,$
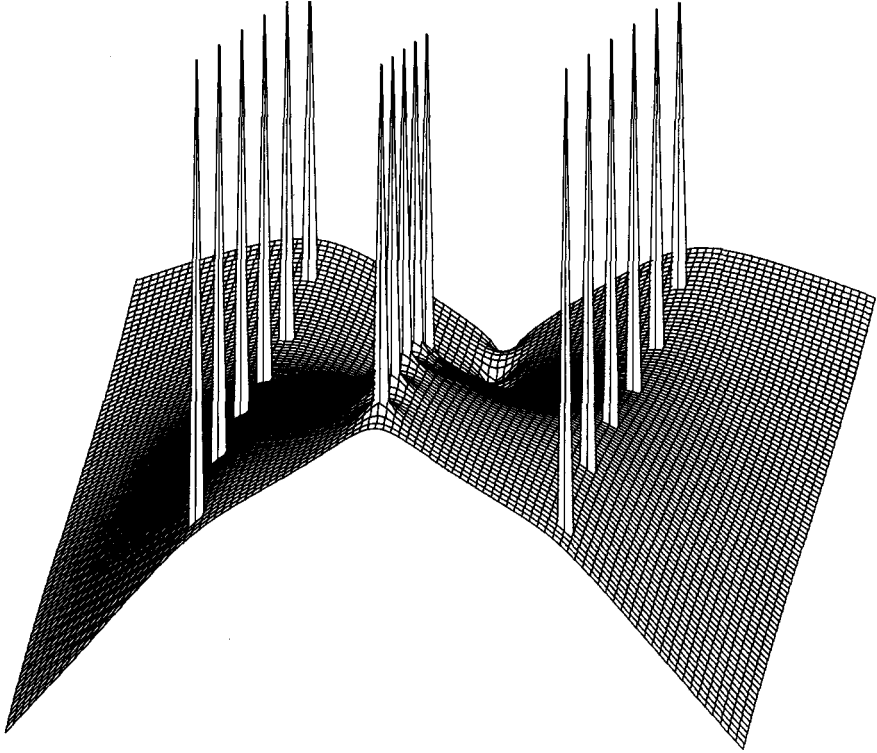
FIG. 10. The logarithm of the absolute value of the integrand in (A1) for $v = 1$, $\omega_0 = \frac{1}{2}\pi$, $s_c = 3/\pi$, $v = 0.8$, $2as_c\,\omega_0 = 1$ (optimized filters). The surface is seen from a point $10°$ from the negative imaginary axis towards the positive real axis, and $10°$ above the complex plane.

$1, 2, \ldots$, where it possesses simple poles with the residues

$$R_n = \mp \frac{a}{2\pi}, \qquad\qquad\qquad\qquad (\text{A5})$$

while $\exp(i2\pi vs)$ is analytic everywhere.

Figure 10 shows the logarithm of the absolute value of the integrand in (A1) seen from a point $10°$ from the negative imaginary axis towards the positive real axis, and $10°$ over the complex plane. The poles are given a finite value for clarity. We see the row of poles of $\hat{H}_v(\xi)$ down the negative imaginary axis and the two rows of poles of $\Delta\hat{P}(\Delta\xi)$.

Consider the contour C_2 (Fig. 2) in the lower half-plane $\xi = s + i\sigma$, $\sigma < 0$. As $\sigma \to -\infty$, $\hat{H}_v(\xi)$ approaches zero faster than any exponential function, $\Delta\hat{P}(\Delta\xi)$ stays bounded outside its poles and $\exp(i2\pi v\xi)$ decreases exponentially for $v < 0$ and increases exponentially for $v > 0$. Thus the integral along the lower horizontal return path vanishes in the limit as $\sigma \to -\infty$ regardless of the sign of v. For fixed σ, $|s| \to \infty$, $\hat{H}_v(\xi)$ decreases as $|\pi s|^{2\pi\sigma}$ in the lower half-plane, $\exp(i2\pi v\xi)$ stays bounded, and $\Delta\hat{P}(\Delta\xi) \sim \exp(-2\pi|s|/2as_c)$, so the integrals along the vertical paths of C_2 vanish in the limit.

We obtain

$$H_v^*(v) = -2\pi i \sum \text{(residues inside } C_2\text{)},$$

$$= -2\pi i \left\{ \sum_{n=0}^{\infty} i(-1)^n \frac{2^{-(2n+v+1)}}{\pi \Gamma(n+1)\Gamma(n+v+1)} \Delta \hat{P}(\Delta z_n) \exp{(i2\pi v z_n)} \right.$$

$$+ \sum_{n=0}^{\infty} -\frac{a}{2\pi} \hat{H}_v[s_c - i2as_c(n+\tfrac{1}{2})] \exp{\{i2\pi v[s_c - i2as_c(n+\tfrac{1}{2})]\}}$$

$$\left. + \sum_{n=0}^{\infty} \frac{a}{2\pi} \hat{H}_v[-s_c - i2as_c(n+\tfrac{1}{2})] \exp{\{i2\pi v[-s_c - i2as_c(n+\tfrac{1}{2})]\}} \right\}.$$

$$\text{(A6)}$$

Substituting z_n in the exponential function and noting that $\hat{H}_v(-\bar{\xi}) = \hat{H}_v(\xi)$, we find that the second and third sums are each others conjugates and we obtain (16)

$$H_v^*(v) = 2^{-v} \exp{[(v+1)v]} \sum_{n=0}^{\infty} \frac{(-1)^n}{4^n \Gamma(n+1)\Gamma(n+v+1)} \exp{(2nv)}\Delta \hat{P}(\Delta z_n)$$

$$- 2a \exp{(2\pi as_c v)} \text{Im} \left\{ \exp(i2\pi s_c v) \sum_{0}^{\infty} \exp{(4\pi as_c nv)}\hat{H}_v(\xi_n^-) \right\}, \qquad \text{(A7)}$$

where

$$s_c = \frac{1}{2\Delta}, \qquad z_n = -\frac{i}{\pi}\left(n + \frac{v+1}{2}\right), \qquad \xi_n^{\pm} = s_c \pm i2as_c(n+\tfrac{1}{2}).$$

Now, consider the contour C_1 (Fig. 2) encircling the upper half-plane $\xi = s + i\sigma$, $\sigma > 0$. As $\sigma \to \infty$, $\hat{H}_v(\xi)$ approaches infinity faster than any exponential function, $\Delta \hat{P}(\Delta \xi)$ stays bounded outside its poles and $\exp{(i2\pi v \xi)}$ increases exponentially for $v < 0$ and decreases exponentially for $v > 0$. Though $\hat{H}_v(\xi)$ increases faster than any exponential function, the exponential decay of $\exp{(i2\pi v \xi)}$ for $v > 0$ introduces a 'valley' in which we may place the horizontal return path in the upper half-plane. The minimum in the valley decreases as v increases, so there exists a certain v^+ such that the integral through the valley becomes negligible for $v > v^+$. For fixed σ, $|s| \to \infty$, $\hat{H}_v(\xi)$ increases as $|\pi s|^{2\pi\sigma}$ in the upper half-plane, $\exp{(i2\pi vs)}$ stays bounded, and $\Delta \hat{P}(\Delta \xi) \sim \exp{(-2\pi|s|/2as_c)}$, so $\hat{H}_v(\xi)$ increases more slowly than $\Delta \hat{P}(\Delta \xi)$ decreases and the integrals along the vertical paths of C_1 vanish in the limit. We obtain

$$H_v^*(v) = 2\pi i \sum \text{(residues inside } C_1\text{)},$$

$$= 2\pi i \left\{ \sum_{n=0}^{N} -\frac{a}{2\pi} \hat{H}_v[s_c + i2as_c(n+\tfrac{1}{2})] \exp{\{i2\pi v[s_c + i2as_c(n+\tfrac{1}{2})]\}} \right.$$

$$\left. + \sum_{n=0}^{N} \frac{a}{2\pi} \hat{H}_v[-s_c + i2as_c(n+\tfrac{1}{2})] \exp{\{i2\pi v[-s_c + i2as_c(n+\tfrac{1}{2})]\}} \right\}.$$

$$\text{(A8)}$$

Again we observe that the second and third sums are each others conjugates and we obtain (17)

$$H^*_\nu(v) = 2a \exp\left(-2\pi a s_c\, v\right) \operatorname{Im}\left\{\exp\left(i2\pi s_c\, v\right) \sum_{n=0}^{N} \exp\left(-4\pi a s_c\, nv\right)\hat{H}_\nu(\xi_n^+)\right\}. \quad (A9)$$

REFERENCES

ABRAMOWITZ, M. and STEGUN, A.S. (eds), 1970. *Handbook of Mathematical Functions.* Dover, New York.

ANDERSON, W.L., 1979. Numerical integration of related Hankel transforms of orders 0 and 1 by adaptive digital filtering. *Geophysics* **44**, 1287–1305.

ANDERSON, W.L. 1982. Fast Hankel transforms using related and lagged convolutions. *Association for Computing Machinery Transactions on Mathematical Software* **8**, 344–368.

ANDERSON, W.L. 1989. A hybrid fast Hankel transform algorithm for electromagnetic modelling. *Geophysics* **54**, 263–266.

BERNABINI, M. and CARDARELLI, E., 1978. The use of filtered Bessel functions in direct interpretation of geoelectrical soundings. *Geophysical Prospecting* **26**, 841–852.

BICHARA, M. and LAKSHMANAN, J. 1976. Fast automatic processing of resistivity soundings. *Geophysical Prospecting* **24**, 354–370.

BRACEWELL, R. 1965. *The Fourier Transform and its Applications.* McGraw-Hill Book Co.

DAS, U.C. and GHOSH, D.P. 1974. The determination of filter coefficients for the computation of standard curves for dipole resistivity sounding over layered Earth by linear digital filtering. *Geophysical Prospecting* **22**, 765–780.

DAS, U.C., GHOSH, D.P. and BIEWINGA, D.T. 1974. Transformation of dipole resistivity sounding measurements over layered earth by linear digital filtering. *Geophysical Prospecting* **22**, 476–489.

GHOSH, D.P. 1971a. The application of linear filter theory to the direct interpretation of geoelectrical resistivity sounding measurements. *Geophysical Prospecting* **19**, 192–217.

GHOSH, D.P. 1971b. Inverse filter coefficients for the computation of apparent resistivity standard curves for a horizontally stratified earth. *Geophysical Prospecting* **19**, 769–775.

GOLDMAN, M. 1987. Forward modelling for frequency domain marine electromagnetic systems. *Geophysical Prospecting* **35**, 1042–1064.

GUPTASARMA, D. 1982. Optimization of short digital linear filters for increased accuracy. *Geophysical Prospecting* **30**, 501–514.

HAINES, G.V. and JONES, A.G. 1988. Logarithmic Fourier transformation. *Geophysical Journal of the Royal Astronomical Society* **92**, 171–178.

JOHANSEN, H.K. 1975. An interactive computer/graphic–display–terminal system for interpretation of resistivity soundings. *Geophysical Prospecting* **23**, 449–458.

JOHANSEN, H.K. and SØRENSEN, K. 1979. Fast Hankel transforms. *Geophysical Prospecting* **27**, 876–901.

KOEFOED, O. 1972. A note on the linear filter method of interpreting resistivity sounding data. *Geophysical Prospecting* **20**, 403–405.

KOEFOED, O. and DIRKS, F.J.H. 1979. Determination of resistivity sounding filters by the Wiener–Hopf Least-Squares Method. *Geophysical Prospecting* **27**, 245–250.

KOEFOED, O., GHOSH, D.P. and POLMAN, G.J. 1972. Computation of type curves for electromagnetic depth sounding with a horizontal transmitting coil by means of a digital linear filter. *Geophysical Prospecting* **20**, 406–420.

NISSEN, J. and ENMARK, T. 1986. An optimized digital filter for the Fourier transform. *Geophysical Prospecting* **34**, 897–903.